Journal of NeuroVirology (2000) 6, 462–477

www.jneurovirol.com

Alterations in neurotrophin and neurotrophin receptor gene expression patterns in the rat central nervous system following perinatal Borna disease virus infection

Marcel Zocher[1,5], Stefanie Czub[2], Jürgen Schulte-Mönting[3], Juan Carlos de la Torre[4] and Christian Sauder*[,1]

[1]*Department of Virology, Institute for Medical Microbiology and Hygiene, University of Freiburg, Hermann-Herder-Str. 11, 79104 Freiburg, Germany;* [2]*Institute of Pathology, University of Würzburg, 97080, Germany;* [3]*Department of Medical Biometry and Statistics, University of Freiburg, Stefan-Meier-Str. 26, 79104 Freiburg, Germany and* [4]*Division of Virology, Department of Neuropharmacology, The Scripps Research Institute, 10550 North Torrey Pines Road, La Jolla, CA 92037, USA*

Infection of newborn rats with Borna disease virus (BDV) leads to persistence in the absence of overt signs of inflammation. BDV persistence, however, causes cerebellar hypoplasia and hippocampal dentate gyrus neuronal cell loss, which are accompanied by diverse neurobehavioral abnormalities. Neurotrophins and their receptors play important roles in the differentiation and survival of hippocampal and cerebellar neurons. We have examined whether BDV can cause alterations in the neurotrophin network, thus promoting neuronal damage. We have used RNase protection assay to measure mRNA levels of the neurotrophins nerve growth factor (NGF), brain-derived neurotrophic factor (BDNF), and neurotrophin-3 (NT-3), and their trkC and trkB receptors, as well as the growth factors insulin-like growth factor I (IGF-1) and basic fibroblast growth factor (bFGF), in the cerebellum and hippocampus of BDV-infected and control rats at different time points p.i. Reduced mRNA expression levels of NT-3, BDNF and NGF were found after day 14 p.i. in the hippocampus, but not in the cerebellum, of newborn infected rats. Three weeks after infection, trkC mRNA expression levels were reduced in both hippocampus and cerebellum of infected rats, whereas decreased trkB mRNA levels were only observed in the cerebellum. Reduced trkC mRNA expression was confined to the dentate gyrus of the hippocampus, as assessed by *in situ* hybridization. TUNEL assay revealed massive apoptotic cell death in the dentate gyrus of infected rats at days 27 and 33 p.i. Increased numbers of apoptotic cells were also detected in the cerebellar granular layer of infected rats after 8 days p.i. Moreover, a dramatic loss of cerebellar Purkinje cells was seen after day 27 p.i. Our results support the hypothesis, that BDV-induced alterations in neurotrophin systems might contribute to selective neuronal cell death. *Journal of NeuroVirology* (2000) **6,** 462–477

Keywords: Borna disease virus; neurotrophins; neurotrophin receptors; neuronal cell death; dentate gyrus; Purkinje cell

Introduction

Congenital and perinatal virus infections of the central nervous system (CNS) can induce neurodevelopmental and neuropsychiatric disorders (Seay and Griffin, 1981; Yolken and Torrey, 1995). Defining the mechanisms, that disturb normal brain structures and functions during infection, can contribute to our understanding of the cellular and molecular basis of environmentally-triggered CNS disorders whose etiology remain elusive.

Borna disease virus (BDV) may induce CNS disease in a broad range of vertebrate animal species. The disease is manifested by behavioral

*Correspondence: C Sauder
[5]Current address: Micromet GmbH, Am Klopferspitz 19, 82152 Martinsried/München, Germany
Received 21 December 1999; revised 30 March 2000; accepted 23 May 2000

abnormalities and diverse pathology (Rott and Becht, 1995; Gosztonyi and Ludwig, 1995). Moreover, serological data and recent molecular epidemiological studies suggest that BDV can infect humans, and might be associated with certain neuropsychiatric disorders. However, BDV has not been implicated as a human pathogen yet (reviewed in Gonzalez-Dunia *et al*, 1997). BDV provides an important model for the investigation of the mechanisms and consequences of viral persistence in the CNS. Studies on this viral system are not only contributing to the elucidation of immune-mediated pathological events involved in virus-induced neurological disease, but also help to understand the mechanisms whereby viruses induce behavioral and neurodevelopmental disturbances in the absence of the hallmarks of cytolysis and inflammation (Gonzalez-Dunia *et al*, 1997). BDV is non-cytolytic and neurotropic, and has been molecularly characterized to be a non-segmented, negative-strand (NNS) RNA virus. Based on its unique genetic and biological features, BDV represents the prototypic member of a new family. Bornaviridae, within the order Mononegavirales (de la Torre, 1994; Schneemann *et al*, 1995).

Experimentally, BDV exhibits a wide host range including species phylogenetically distant from birds to rodents and non-human primates (Rott and Becht, 1995). The clinical outcome of BDV infection depends on viral factors, as well as on the genetics and immune status of the host. Intracerebral infection of rats within 24 h post partum causes persistence in the absence of clinical symptoms and of gross immune cell infiltration in the CNS (Hirano *et al*, 1983; Narayan *et al*, 1983). These rats, designated PTI-NB (persistent tolerant infection of the newborn) exhibit distinct cognitive, behavioral, physiological and neuroanatomical abnormalities (Dittrich *et al*, 1989; Carbone *et al*, 1991; Bautista *et al*, 1994; Rubin *et al*, 1998b; Pletnikov *et al*, 1999a,b). Cerebellar hypoplasia and progressive degeneration of the hippocampal dentate gyrus (DG) granule neurons together with prominent astrocytosis and microgliosis are the histopathological hallmarks observed in PTI-NB rats (Carbone *et al*, 1991; Bautista *et al*, 1995; Sauder and de la Torre, 1999). Interference of BDV with the development of brain regions that undergo postnatal maturation, such as cerebellum and hippocampus, has been postulated to trigger neuronal damage (Bautista *et al*, 1995). However, the cellular and molecular mechanisms underlying BDV-induced cerebellar hypoplasia and DG degeneration are hitherto unknown.

Cerebellar and hippocampal granule cell maturation and survival is largely influenced by neurotrophic and growth factors including NT-3, BDNF, IGF-I and bFGF (reviewed in Connor and Dragunow, 1998; Lewin and Barde, 1996; Lindholm *et al*, 1997; Tessarollo, 1998). Studies using neurotrophin- and neurotrophin-receptor knockout mice have shown that the majority of neurotrophin responsive CNS neurons are able to survive in the absence of a single neurotrophin or its cognate receptor (Snider, 1994). However, double-knockout mice devoid of both functional trkB and trkC, the receptors for BDNF and NT-3, respectively, displayed increased neuronal cell death of cerebellar and hippocampal granule cells, indicating that trkC and trkB cooperatively promote survival of these cells (Minichiello and Klein, 1996). Furthermore, BDNF or NT-3 knockout mice display abnormal cerebellar development, which in case of BDNF, involved increased cerebellar granule cell loss (Schwartz *et al*, 1997; Bates *et al*, 1999). We therefore sought to examine the hypothesis that virus-mediated interference with neurotrophins and their receptor network systems might contribute to neuronal cell loss and developmental damage in the PTI-NB rat brain. Here we show that mRNA levels of NGF, NT-3 and BDNF are significantly decreased in hippocampus, but not in cerebellum, of BDV PTI-NB rats. In addition, we found reduced levels of transcripts encoding both full-length and truncated trkC-receptor genes in the hippocampus and cerebellum of infected rats. Furthermore, trkB mRNA levels were also reduced in the cerebellum of infected rats. We also observed cerebellar Purkinje cell loss in the PTI-NB rat brain starting at 27 days p.i. Results from TUNEL assays indicated that BDV-induced decrease in neurotrophin and neurotrophin receptor expression preceded the onset of neuronal cell death, supporting a role of neurotrophins in BDV induced brain damage.

Results

Reduced neurotrophin mRNA expression in hippocampus, but not in cerebellum, of PTI-NB rats

To measure RNA expression of selected neurotrophins and growth factors in the rat CNS, we developed a multiprobe set suitable for RNase protection assay (RPA). This probe set included the rat neurotrophins NT-3, BDNF, β-NGF, as well as the growth factors bFGF and IGF-I (Table 1). The riboprobe s*et al*so included a probe to detect RNA levels of the housekeeping gene ribosomal protein L32. Neurotrophin and growth factor mRNA expression was normalized with respect to L32 RNA levels. Total RNA from hippocampus and cerebellum of BDV PTI-NB and control rats was prepared at days 8, 14, 21, 27, 33 and 48 p.i., and analyzed by RPA. In a first set of experiments, RNA from two to three rats per group and time point was analyzed. We did not observe statistically significant differences between the two groups over the entire timecourse in cerebellar mRNA expression levels of BDNF, NT-3, bFGF and IGF-I, as determined by two-way ANOVA (data not shown). Cerebellar NGF levels were below detection limit in our RPA.

Table 1 Specifications of plasmids used for RPA and ISH studies.

Gene	*Subcloned sequence (position in gene)*	*Length*	*Polymerase and restriction enzyme used for antisense transcript*	*GenBank accession no.*	*Reference*
β-NGF	347–645	299	T7/*Hind*III	M36589	Whittemore *et al*., 1988
NT-3	334–531	198	T7/*Hind*III	M33968	Maisonpierre *et al*., 1990
BDNF	196–376	181	T7/*Hind*III	M61175	Maisonpierre *et al*., 1991
bFGF	89–253	164	T7/*Hind*III	E04331	Koichi *et al*., unpublished
IGF-I	32–168	137	T7/*Hind*III	X06043	Murphy *et al*., 1987
trkC-Kin	2132–2375	244	T7/*Hind*III	L14447	Valenzuela *et al*., 1993
trkC-Ex	821–1327	507	T7/*Hind*III (SP6/*Eco*RI)[a]	L14447	Valenzuela *et al*., 1993
trkB-Kin	2697–2918	222	T7/*Hind*III	M55291	Middlemas *et al*., 1991
RPL32N	1219–1293 and 1931–1954	99	T7/*Hind*III	K02060	Dudov and Perry, 1984

[a]Polymerase and restriction enzyme used to generate sense transcript.

In contrast to the situation in the cerebellum, mRNA levels of NGF, NT-3 and BDNF were significantly reduced in hippocampus of PTI-NB rats compared to controls over the entire timecourse, as determined by two-way ANOVA (Figure 1A). Hippocampal IGF-I mRNA levels were similar in PTI-NB and control rats, except for day 33, where PTI-NB rats exhibited about a 100% increase compared to controls (Figure 1A). Levels of NT-3, BDNF and NGF mRNA appeared to first decrease in the hippocampi of PTI-NB rats compared to control rats already at day 21 p.i. (Figure 1A). However, the limited number of rats analyzed per time point precluded statistical analysis of data for individual time points. To address this question, we performed RPA with RNA samples prepared from the hippocampi of five rats each per group and time point (days 14, 21, and 27 p.i.) (Figure 1B). Statistical data analysis by two-way ANOVA indicated that the overall differences between the two groups over the entire timecourse for NGF, BDNF and NT-3 mRNA levels achieved statistical significance (Table 2). Subsequent comparison of the neurotrophin gene expression levels between the two groups at the individual time points using a *post-hoc* one-way ANOVA revealed statistically significant reduced levels for hippocampal NGF, BDNF and NT-3 gene expression in PTI-NB rats compared to control rats at days 21 and 27 p.i. (Table 3). No differences in IGF-I levels between the two groups were found at the three time points (Tables 2 and 3). In contrast, bFGF mRNA levels were significantly reduced in the hippocampus of PTI-NB rats at day 21 p.i. (1.4-fold reduction), but not at days 14 and 27 p.i. (Tables 2 and 3).

mRNA expression levels of trkC- and trkB-neurotrophin receptors are altered in the PTI-NB rat brain

Having found a significant decrease in hippocampal mRNA expression levels of the neurotrophins NT-3, BDNF and NGF in the PTI-NB rat, we next asked whether the expression patterns of the corresponding neurotrophin receptors were also altered following BDV infection. We focused on the analysis of tyrosine kinases trkC and trkB, which represent the primary receptors for NT-3 and BDNF, respectively. Both trkB and trkC are highly expressed in the rat hippocampus (Lindsay *et al*, 1994). Rat trkB and trkC exist in different isoforms, some of which code for truncated receptors that lack the intracytoplasmic kinase domains (reviewed in Tessarollo, 1998). Some other isoforms of trkC contain amino acid (aa) insertions within the tyrosine kinase domain. Insertions of either a 14 aa motif, a 25 aa motif, or both have been described, being designated as trkC ki14, trkC ki25, and trkC ki39, respectively. The full-length isoform lacking insertions is the most abundant in the rat brain (Tsoulfas *et al*, 1993; Valenzuela *et al*, 1993). To measure mRNA expression of the different trkC isoforms, we performed RPA using a probe similar to that described by Valenzuela *et al* (1993), which covers part of the kinase domain region and includes both insertion motifs (Figure 2A). This probe enabled us the detection of trkC, trkC ki14, and trkC ki39 isoforms, but did not allow a distinction between trkC and trkC ki25 isoforms. Nonetheless, trkC ki25 comprises only 5% of the amount of all isoforms present in rat brain (Tsoulfas *et al*, 1993). Thus, changes in the intensities of RPA signals assigned to trkC and trkC ki25 isoforms are rather attributable to changes in trkC-, than in trkC ki25-expression.

Total RNA from hippocampus and cerebellum of PTI-NB and control rats prepared at different time points p.i. (2–3 animals per group and time point) was analyzed by RPA using the trkC probe described above (Figure 2, and data not shown). Consistent with a previous report (Valenzuela *et al*, 1993), the trkC isoform was the most abundant in cerebellum and hippocampus from both PTI-NB and control rats. Isoform trkC ki39 was very weakly expressed, and we therefore excluded it from

subsequent quantitative analysis. Using two-way ANOVA, we measured statistically significant overall differences between the two groups over the entire timecourse in cerebellar and hippocampal expression levels of trkC ki14 and trkC/trkC ki25 receptor isoforms (Figure 2, and data not shown;

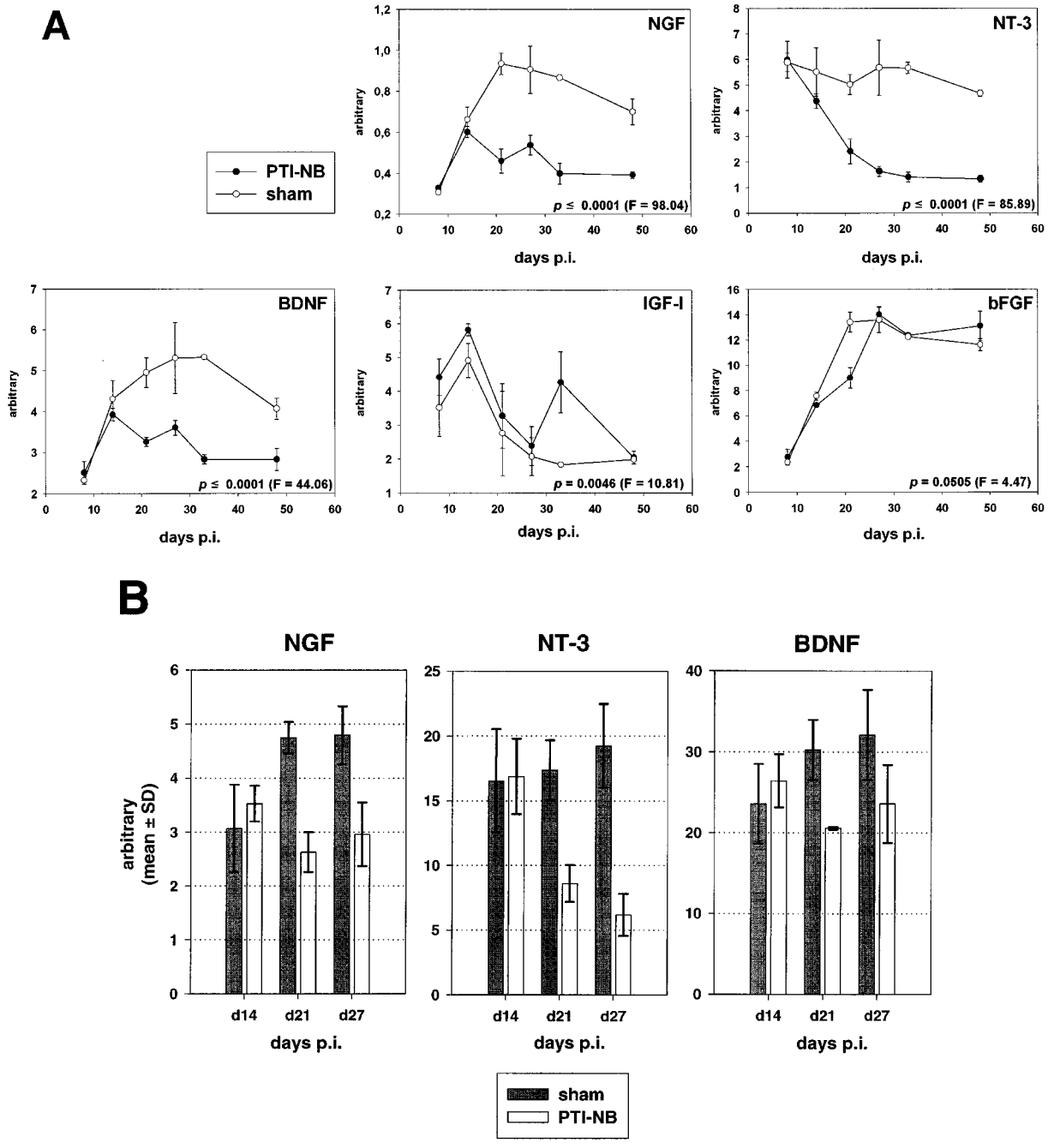

Figure 1 Semiquantitative analysis of neurotrophin and growth factor gene expression in the hippocampus of PTI-NB and control rats. Total RNA (10 μg) from hippocampus of neonatally sham-infected or BDV-infected (PTI-NB) rats, sacrificed at different days p.i., was subjected to RPA using the neurotrophin/growth factor probe as described in Materials and methods. (**A**) Two to three animals per group and time point each were used for RPA; (**B**) Five animals per group and time point each were used for RPA. For quantitation, the dried RPA gels were exposed to phosphoimager plates and band intensities were quantified using MacBAS software. Dots in (**A**) and bars in (**B**) indicate mean values $\pm$ standard errors and mean values $\pm$ standard deviations (s.d.), respectively, per time point p.i. (in days) after normalization against L32 expression levels (values represent arbitrary units). (**A**) To test whether overall differences in trophic factor mRNA levels between the two groups over the entire timecourse achieve statistical significance, two-way ANOVA was used (α=0.05). Group effect *P*- and *F*-values are indicated in the respective graphs. Degrees of freedom were one each. See Tables 2 and 3 for statistical analysis of data depicted in (**B**).

Table 2 Comparison of hippocampal neurotrophin gene expression levels between PTI-NB and control rats over a period of three time points (days 14, 21 and 27 p.i., n=5 per group and time point) using two-way ANOVA (logarithmic).

Trophic factors analyzed	P- *and* F-*values*	*Two-way ANOVA*[a]		
		Group effects	*Day effects*	*Group × day effects*
NGF	*F*=	22.11	1.66	13.69
	P=	0.0001	0.2115	0.0001
NT-3	*F*=	63.98	11.06	20.83
	P=	0.0001	0.0004	0.0001
BDNF	*F*=	9.39	1.03	6.82
	P=	0.0053	0.3708	0.0045
IGF-I	*F*=	1.38	20.99	0.78
	P=	0.2523	0.0001	0.4682
bFGF	*F*=	10.4	86.29	12.61
	P=	0.0036	0.0001	0.0002

[a]Degrees of freedom are one each for group effects and two for day and group × day effects, respectively.

Table 3 Comparison of hippocampal neutrophin gene expression levels between PTI-NB and control rats at three individual time points p.i. (n=5 per group and time point), using a *post-hoc* one-way ANOVA (logarithmic).

Days p.i.	P- *and* F-*values*[a]	*Trophic factors analyzed*				
		NGF	*NT-3*	*BDNF*	*IGF-I*	*bFGF*
14	*F*=	1.3	0.06	1.12	0.81	1.31
	P=	0.2865	0.8124	0.3212	0.3932	0.2858
21	*F*=	69.21	48.2	34.92	0.03	68.02
	P=	0.0001	0.0001	0.0004	0.8594	0.0001
27	*F*=	23.35	71.67	6.59	2.7	2.01
	P=	0.0013	0.0001	0.0333	0.139	0.1938

[a]Degrees of freedom are one each.

group effect P-values were $\leqslant 0.0001$ for all isoforms). We performed additional RPA using total hippocampal RNA from each five rats per group and time point (days 14, 21 and 27 p.i.) (data not shown). Two-way ANOVA revealed an overall statistically significant difference between the two groups over the three time points for the trkC ki14 and trkC/trkC ki25 isoforms (data not shown). Applying a *post-hoc* one-way ANOVA which compared receptor levels between the groups at individual time points, we could verify that the decline of trkC ki14 and trkC/trkC ki25 mRNA levels in the PTI-NB rat brain achieved statistical significance at day 21 and 27 p.i. (P- and F-values for trkC ki14 and trkC/trkC ki25 were $P \leqslant 0.0001$ (F=63.22) and P=0.0004 (F=33.51), respectively, for day 21 p.i. and $P \leqslant 0.0001$ (F=99.59) and P=0.0004 (F=33.18), respectively, for day 27 p.i.; degrees of freedom were one for each time point).

We next performed RPA using a probe covering a region of the trkC gene which codes for the extracellular domain of the trkC receptor (trkC-Ex). In this case, RPA signals reflect the combined expression levels of all receptor isoforms, including the truncated versions. We observed a significant overall difference in hippocampal and cerebellar trkC RNA expression levels between PTI-NB and control rats over the entire timecourse as determined by two-way ANOVA (Figure 2; n=2–3 rats per group and time point). Expression levels of trkC-Ex appeared to be already reduced by day 14 p.i. in the hippocampus, and by day 21 in the cerebellum.

Whereas trkC and trkB receptor isoforms lacking the respective kinase domain are expressed both in neurons and astrocytes, functional full-length receptor isoforms were found to be exclusively expressed in neurons (Valenzuela *et al*, 1993). To analyze neuronally expressed full-length trkB, we performed RPA using a probe covering part of the trkB tyrosine kinase domain (trkB-kin). We did not observe statistically significant overall differences between PTI-NB and control rats in hippocampal trkB-kin expression levels (Figure 2). In contrast, using two-way ANOVA, a significant overall difference in cerebellar trkB-kin mRNA levels was observed between PTI-NB and control rats, with reduced trkB-kin mRNA levels in the PTI-NB rats after day 14 p.i. (Figure 2).

Reduced trkC mRNA expression is confined to the dentate gyrus region in the hippocampus of PTI-NB rats

With the aim to identify the subset of brain cells with decreased expression of trkC mRNAs in PTI-NB rats, we performed *in situ* hybridization (ISH) studies using the trkC-Ex probe described above. Paraffin-embedded brain sections from PTI-NB and control rats, sacrificed at different time points p.i., were prepared. BDV infection was confirmed by IHC using a monoclonal antibody against the BDV nucleoprotein (data not shown). Control rat brains exhibited the previously characterized regional distribution of trkC expression (Merlio *et al*, 1992). Thus, cerebellum, neocortex and hippocampus displayed high levels of trkC ISH signals (Figure 3A). In hippocampus, labeling was strongest in the DG granule cell layer followed by the pyramidal cell layer. In the cerebellum, cells of the granule- and Purkinje cell layer were labeled. Hybridization with a trkC-Ex sense probe did not yield specific signals validating the specificity of the trkC antisense probe (data not shown). We observed a clear reduction in the intensity of ISH signals, restricted to the DG region, in PTI-NB compared to sham infected control rat brains. This decrease became evident by day 27 p.i. and progressed until day 48 p.i., the last time point investigated (Figure 3A,B). The decrease of trkC ISH signals in the infected brains paralleled the progressive loss of DG granule neurons (Figure 3B). Comparison of ISH signals in cerebelli of PTI-NB rats and controls did not reveal

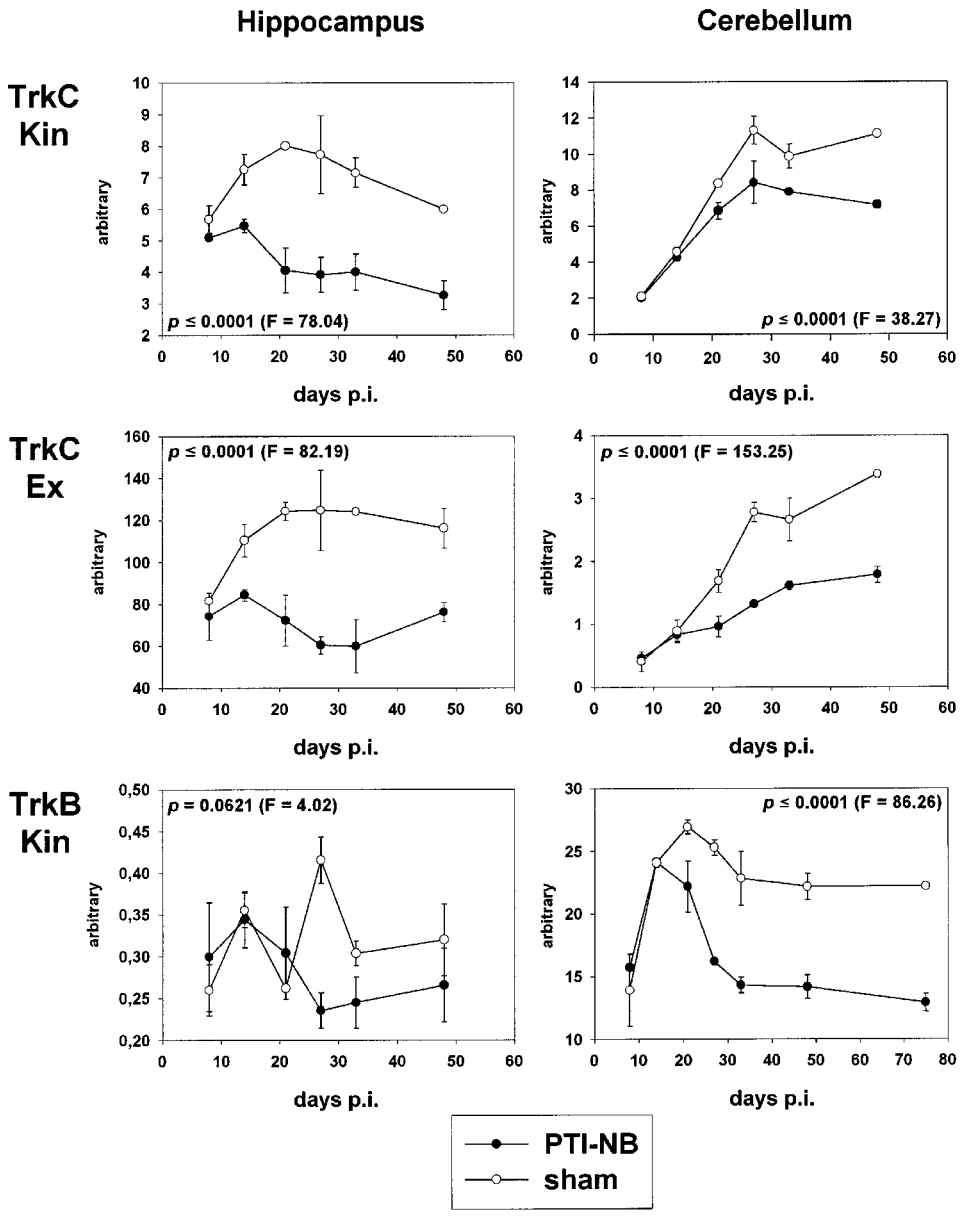

Figure 2 Semiquantitive analysis of trkC and trkB receptor gene expression in hippocampus and cerebellum of PTI-NB and control rats. Total RNA (10 μg) prepared from the hippocampi and cerebelli of neonatally sham-infected or BDV-infected (PTI-NB) rats, sacrificed at different days p.i. (two or three animals per group and time point), was subjected to RPA using probes trkC-kin, trkC-Ex and trkB-kin, as described in Materials and methods. See Results section for further information on probes. RPA gels were dried, exposed to phosphoimager plates and band intensities were quantified using MacBAS software. In case of trkC-kin, the depicted quantitations represent amounts of both full-length trkC gene transcripts as well as transcripts of the full-length trkC gene coding for the receptor which carries the 25 amino acid insertion in the kinase domain (trkC-ki25; see Results section for further information). For further information on graphs, see legend of Figure 1A. To test whether overall differences in receptor mRNA levels between the two groups over the entire timecourse achieve statistical significance, two-way ANOVA was used (α=0.05). Group effect *P*- and *F*-values each are indicated in the graphs. Degrees of freedom were one each.

differences at any of the time points investigated (Figure 3A, and data not shown).

Detection of neuronal apoptosis in the PTI-NB rat brain

Reduced expression levels of neurotrophins and their receptors might trigger or follow neuronal cell loss observed in PTI-NB rats. In the first case, it would be expected that disturbances in the neurotrophin network would precede or parallel the onset of neuronal loss. Neuronal cell death in the PTI-NB rat brain is very restricted, despite BDV being widely distributed within the CNS. In addition, necrotic neurons are not

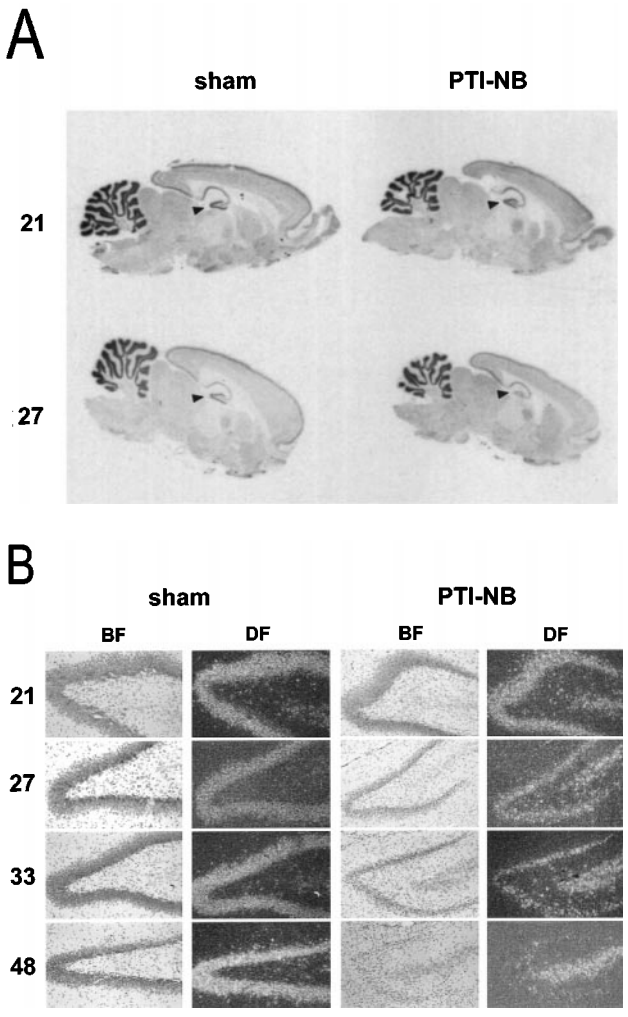

Figure 3 Cellular distribution of the trkC receptor mRNA in the CNS of PTI-NB and control rats. Neonatally sham or BDV (PTI-NB) infected rats were sacrificed at different time points p.i. (indicated on the left in days; **A** and **B**). Following perfusion with 4% PFA, brains were removed, dehydrated and embedded in paraffin. Sagittal sections derived from these brains were probed with a ^{33}P labeled antisense riboprobe covering part of the rat trkC receptor gene, which encodes the extracellular receptor domain. ISH was done as described in the Materials and methods section. (**A**) Scanned autoradiographs after 4 days exposure to film. For each time point, sections from two PTI-NB and two control rats were analyzed. Sections from a PTI-NB and a control rat from the same time point p.i. were mounted on the same slide. Note strong ISH signals in the cerebellar granule layers, the neocortex and hippocampus. Position of the DG is indicated by arrowheads. (**B**) DG sections of PTI-NB and sham infected rats at different time points p.i. Pictures were taken using both bright field (BF) and dark field (DF) microscopy. Original magnification was $\times 20$. Note the progressive degeneration of the DG neurons (BF) paralleled by a decrease in trkC ISH signals (DF) beginning at day 27 p.i. in the PTI-NB rat brain. Expression of trkC in hippocampal CA4 region was not affected by virus, hence the strong ISH signals.

readily observed, suggesting that programmed cell death may be responsible for the neuronal loss observed in the PTI-NB rat brain. We performed TUNEL assays on paraffin embedded sections from two PTI-NB and control rats each, at different time points p.i.. Using this approach, we identified stained nuclei in the brains of both PTI-NB and control rats, indicative of apoptotic cell death (Figure 4A). The number of apoptotic cells in the hippocampus of sham infected rats was very low at all time points analyzed, representing the normal maturation process of the brain. Until day 21 p.i., hippocampal apoptotic cell numbers in PTI-NB rats were only slightly elevated compared to controls, but their numbers strongly increased by day 27 p.i. and peaked at day 33 p.i. (Figure 4A,B). By day 48 p.i., a considerable drop in apoptotic cell number occurred in the hippocampus of PTI-NB rats (Figure 4B). In the cerebellar granule layers, numbers of apoptotic cells were found to be highest at day 8 p.i., with no differences between PTI-NB and control rats (mean of 12.5 cells per counted microscopic field at a $250\times$ magnification; data not shown). In both PTI-NB and control rat cerebelli, apoptotic cell numbers steadily decreased after day 8 p.i. This observation is consistent with the notion, that naturally occurring apoptotic cell death in the rodent cerebellum peaks around postnatal day 8 (Wood *et al*, 1993). However, between days 14 and 48 p.i., apoptotic granule cell numbers were found to be between 2–6-fold higher in PTI-NB rats compared to control rats (data not shown).

Decrease in cerebellar Purkinje cell numbers in PTI-NB rats after day 27 p.i.

Using the TUNEL assay, we did not detect apoptotic cells in the Purkinje cell (PC) layer at any time point examined. However, a significant drop (75%) in the number of PC in the PTI-NB rat brain at 7 months p.i. has been recently described (Eisenman *et al*, 1999). To determine the time point when PC loss first becomes evident, we performed IHC on paraffin-embedded sections from PTI-NB and sham infected control rats at different time points p.i., employing a monoclonal antibody to calbindin D28K, a marker for PC (Figure 5). Until day 27 p.i., we could not observe obvious alterations in the integrity of the PC layer in PTI-NB rats compared to control rats. Gaps in the PC layer of PTI-NB rats appeared to slightly increase by day 27 p.i., and a considerable loss in the PC number was clearly detectable by day 33 p.i.. It should be noted, however, that the extent of PC loss at this time point varied between different cerebellar folia of the same animal. By day 135 p.i., the last time point investigated, very few PC were left in the PTI-NB rat brain (Figure 5 and data not shown). Consistent with previous reports, immunohistochemical staining with an anti BDV p40 antibody revealed early BDV infection of PC, beginning on day 8 p.i. (Bautista *et al*, 1995).

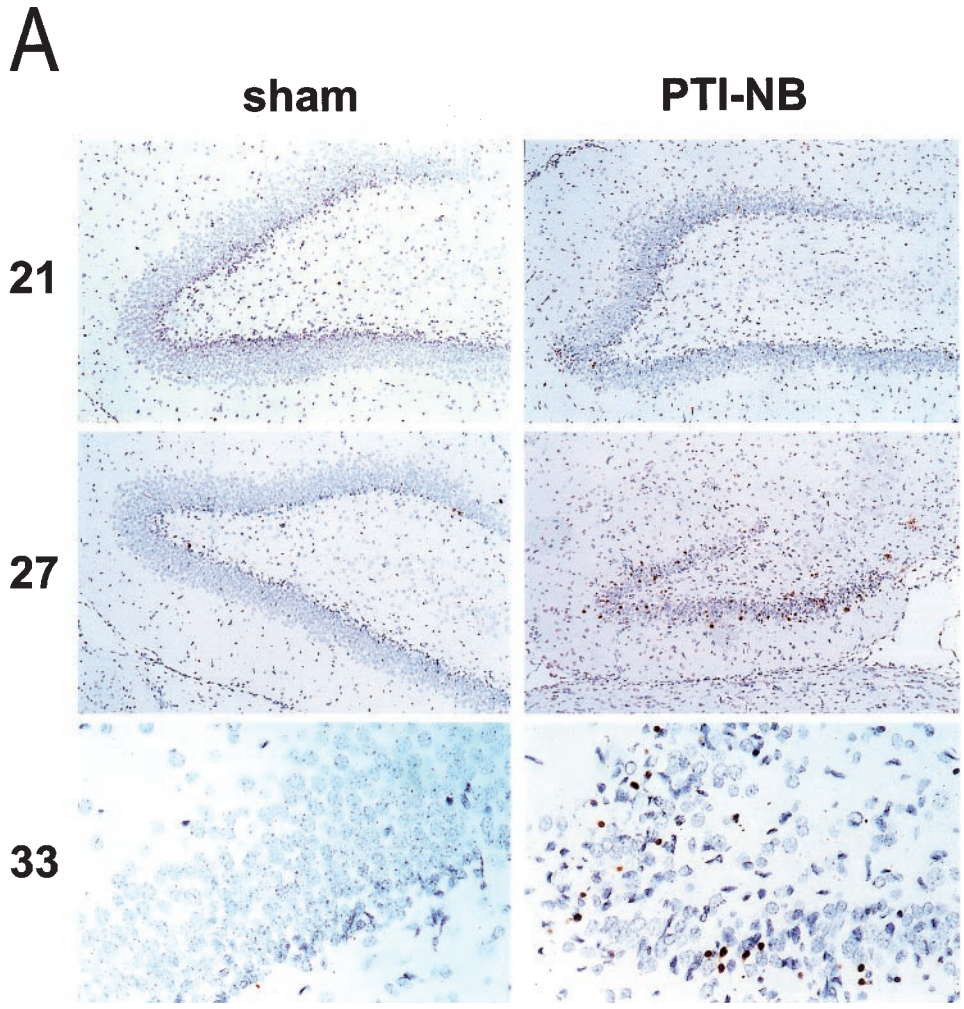

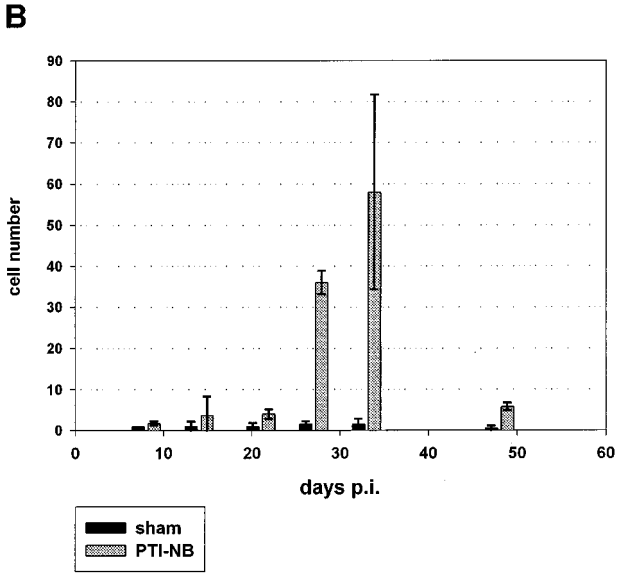

Figure 4 (**A**) Detection of apoptosis in the hippocampus of PTI-NB and control rats. Neonatally BDV-(PTI-NB) and sham-infected rats were sacrificed at different time points p.i. (indicated in days on the left). Following perfusion of rats with 4% PFA, brains were removed and processed for analysis by TUNEL assay as described in Materials and methods. Depicted are DG sections at different days p.i. (magnification: ×80 for days 21 and 27; ×200 for day 33 p.i.). Brown stained nuclei are indicative of cells undergoing apoptosis. (**B**) Quantitative analysis of DG apoptosis. Total numbers of apoptotic cells per slide were counted in the DG of each two PTI-NB and two control rats sacrificed at different time points p.i. Bars represent mean numbers of counted cells ± standard error of mean.

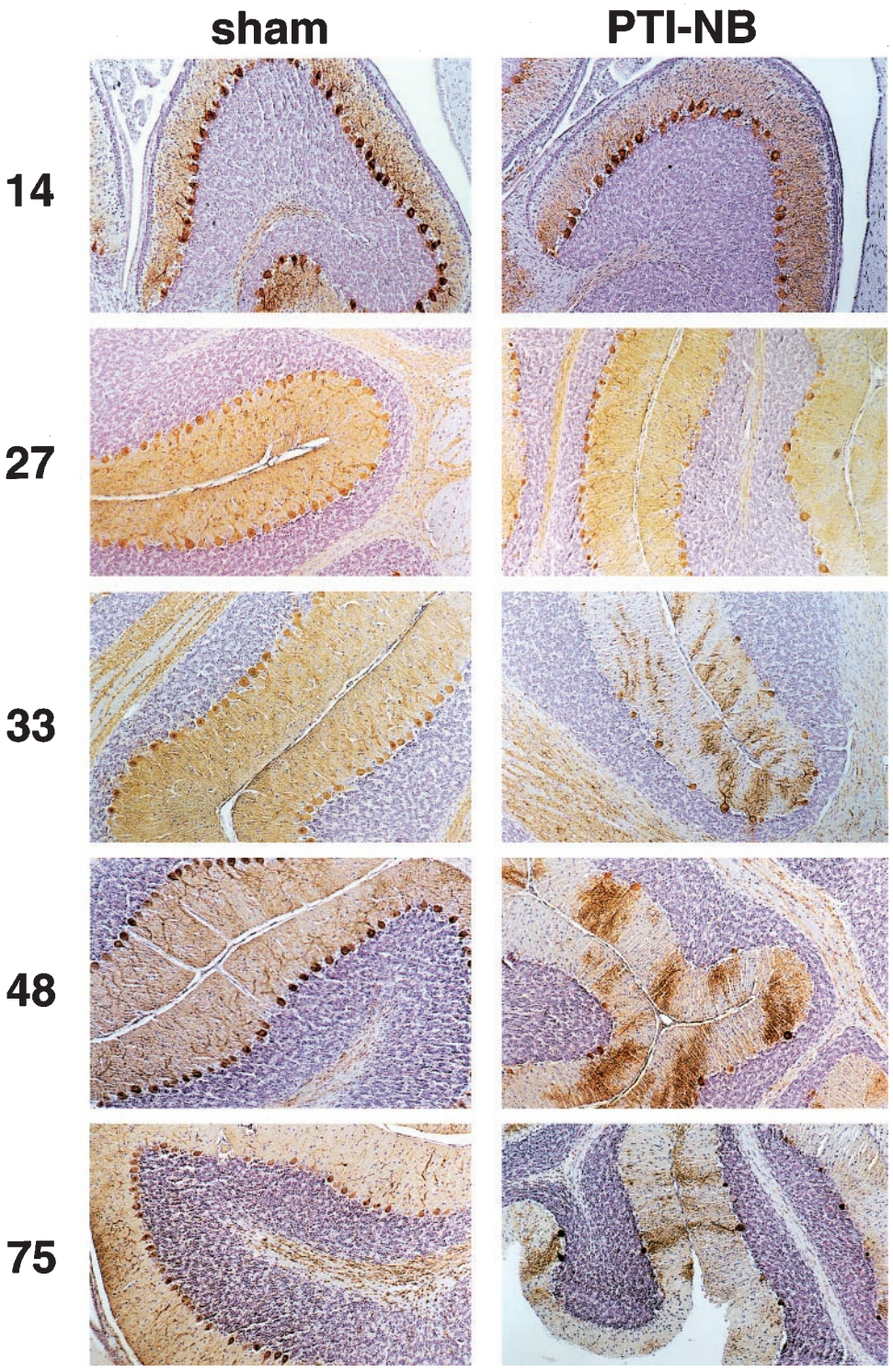

Figure 5 Kinetics of PC loss in the PTI-NB rat brain. Neonatally BDV (PTI-NB) or sham infected rats were sacrificed at different time points p.i. (indicated in days on the left). Following perfusion of rats with 4% PFA, brains were removed and processed for analysis by IHC as described in Materials and methods, using a mAb to rat calbindin-D28K as a marker for PC. Note the homogenous brown stain of the molecular layer in all sham infected animals and PTI-NB rats at days 14 and 27, reflecting staining of PC dendrites. Due to the loss of PC in the PTI-NB rats, staining of dendritic trees of individual PC cells becomes visible in the molecular layers at days 33, 48 and 75 p.i. Sections were counterstained with hematoxylin. Original magnification: $\times 80$.

Discussion

DG degeneration and cerebellar hypoplasia in the PTI-NB rat brain have been attributed to a loss of granule cells in the respective regions. BDNF, bFGF and, to a lesser extent, NT-3, increase both survival and differentiation of rat dentate granule neurons (Lowenstein and Arsenault, 1996). Moreover, previous studies using cultured hippocampal neurons have emphasized the importance of IGF-I, BDNF, NT-3 and neurotrophin-4 (NT-4) for hippocampal neuronal survival (Ip *et al*, 1993; Lindholm *et al*, 1996). However, BDNF or NT-3, as well as trkB or trkC single knockout mice did not exhibit signs of significant hippocampal cell loss, suggesting that the lack of a single component of the neurotrophin network may be compensated by other network components *in vivo* (Henderson, 1996; Snider, 1994). Interestingly, double mutant mice devoid of functional trkC and trkB receptors display massive cell death of postnatal hippocampal and cerebellar granule neurons (Minichiello and Klein, 1996). Assuming that reduced neurotrophin/receptor expression contributes to BDV induced granule cell loss, we reasoned that the former event should precede, or parallel, the latter. Using a TUNEL assay, we observed marked increase in apoptotic granule neurons in the infected hippocampus at day 27 p.i., and after day 8 p.i. in the infected cerebellum, but PC loss was found to take place after day 27 p.i. In the hippocampus, significantly decreased mRNA levels of NT-3, BDNF and NGF were detected first at day 21 p.i. Our results also revealed an early drop, beginning at day 21 p.i., in hippocampal expression levels of trkC NT-3 receptor isoforms. ISH studies indicated that reduced hippocampal trkC Ex expression was restricted to the DG. This was evident only at day 27 p.i., about 1 week later than expected based on the RPA results. Based on the quantitation of RPA data, the difference in trkC Ex expression levels measured between PTI-NB and control rats at day 21 p.i. was relatively small (approximately 1.7-fold). However, ISH signals for trkC Ex were not quantitated. This, together with our observation of a certain degree of section to section and in section variability in the intensities of ISH signals from the same animal, might explain the discrepancy between RPA and ISH data at day 21 p.i. In addition, since rats analyzed by ISH were not identical to those used for RPA studies, and since only a limited number of rats was analyzed by ISH (two animals per group and time point), comparison of ISH data with RPA results is complicated.

We observed a slight decrease in hippocampal levels of trkB RNA in PTI-NB rats after day 21 p.i., which was not statistically significant under our assay conditions. It should be noted, that DG expression levels of trkB-kin were reported to be similar to those found in hippocampal CA1-CA3 regions. In contrast, hippocampal trkC-kin expression levels are highest in the DG neurons (Merlio *et al*, 1992; Valenzuela *et al*, 1993; Ip *et al*, 1993; Figure 4A). Therefore, a reduction of trkB mRNA levels in the PTI-NB rat brain confined to the DG region, as seen for trkC expression, would not be readily detectable by RPA. Expression of BDNF, one of the two ligands of trkB, was reduced in the PTI-NB rat hippocampus. Whether hippocampal expression of NT-4, the other ligand for trkB, is also affected, remains to be determined. Taken together, our data indicate that in the PTI-NB rat hippocampus, reduced expression of NT-3, BDNF and trkC preceded, or at least paralleled, granule cell loss. This, in turn, supports the hypothesis that BDV-induced disturbances in the neurotrophin system can contribute to DG degeneration. The mechanisms whereby BDV interferes with the expression of these molecules are unknown. BDV infects both the pyramidal CA1-CA4 layer and DG neurons in the hippocampus. DG neurogenesis takes place well into adulthood (Gould and McEwen, 1993). The selective vulnerability of DG neurons and its neurotrophin expression patterns to BDV infection might be related to the specific intracellular milieu of these cells, different from differentiated postmitotic neurons (see also Griffin and Hardwick, 1999).

Expression levels of hippocampal IGF-I were increased at day 33 p.i. in PTI-NB rats compared to controls. In rats, constitutive IGF-I hippocampal expression has been shown to be restricted to pyramidal and DG neurons. Upon various insults, such as mechanically or colchicine induced hippocampal injury, a prominent increase in IGF-I mRNA levels is found within the lesioned areas (Garcia-Estrada *et al*, 1992; Breese *et al*, 1996). Microglia and/or activated astrocytes were determined to be the cellular source of this increased IGF-I mRNA expression. We and others have previously shown massive astrocytosis and gliosis of microglia in the PTI-NB rat brain. Within the hippocampus, astrocytosis was most prominent in the DG region once its degeneration started (Carbone *et al*, 1991; Sauder and de la Torre, 1999). The sharp increase in hippocampal IGF-I mRNA levels observed in PTI-NB rats at day 33 p.i. was likely to be mediated by activated astrocytes and microglia surrounding the degenerating DG. This, in turn, could reflect a regenerative response of the brain to neuronal degeneration. Since bFGF has been shown to exert trophic effects on neurons in the dentate gyrus during development and after injury *in vivo* and *in vitro* (see Lowenstein and Arsenault, 1996, and references therein) the significant decrease in bFGF expression levels at day 21 p.i. in the PTI-NB hippocampus might contribute to DG degeneration. However, it remains unclear, why no significant changes in bFGF expression levels were found after day 21 p.i.

In addition to neurotrophins, other factors, including excitatory amino acids and adrenal steroids, are known to regulate neurogenesis in the rat DG (Gould and McEwen, 1993). Disturbances affecting these molecules, as well as a reported sustained upregulation of proinflammatory cytokines (Sauder and de la Torre, 1999; Plata-Salaman *et al*, 1999; Hornig *et al*, 1999), might contribute to DG degeneration.

Selective DG degeneration has also been observed following intracerebral infection of rats with lymphocytic choriomeningitis virus (LCMV) at 4 days of age (Monjan *et al*, 1973). In this case, it has been proposed that hyperexcitability of granule cell neurons eventually triggers neuronal cell loss (Pearce *et al*. 1996). This hyperexcitability is thought to be a consequence of LCMV mediated disturbances in GABA interneurons.

Cerebellar hypoplasia in the PTI-NB rat has been found to correlate with a premature loss of the external granule cell layer and thinning of the internal granular cell layer, which became evident by day 14 p.i. (Bautista *et al*, 1995). These BDV-induced cerebellar defects depend on the maturation state of the cerebellum at the time of infection. Thus, cerebellar damage was no longer observed, when rats were infected at 15 days of age, once cerebellar development is largely completed (Rubin *et al*, 1999). BDV does not appear to infect cerebellar granule cells, whereas Bergmann glia can become infected after 30 days p.i. (Bautista *et al*, 1995; Gosztonyi and Ludwig, 1995). PC are the first cerebellar cells targeted by BDV, becoming infected by day 8 p.i. Cerebellar granule cell neurogenesis and survival depends on PC integrity during an early, critical postnatal period (Smeyne *et al*, 1995). Thus, PC loss before postnatal day 15 leads to massive granule cell loss both in the mouse mutants lurcher (Herrup, 1983) and staggerer (Caddy and Biscoe, 1979), as well as in transgenic mice where PC were ablated due to specific expression of diphteria toxin (Smeyne *et al*, 1995). In contrast, PC loss after postnatal day 15 has no overt impact on the granule cell layer in the mouse mutant pcd (Mullen *et al*, 1976). Our results showed that the onset of PC loss occurs via undefined mechanisms between days 27 and 33 p.i. Therefore, it seems unlikely that increased granule cell loss, observed after day 8 p.i., is due to loss of PC. Alternatively, BDV could also impair PC and/or astrocyte functions required for cerebellar granule cell migration and maturation.

Neurotrophins and their receptors play a crucial role in cerebellar development (see Lindholm *et al*, 1997, for review). Thus, BDNF single knockout mice as well as NT-3 conditional mutants revealed abnormal cerebellar development and foliation (Schwartz *et al*, 1997; Bates *et al*, 1999). BDNF knockout mice displayed increased death of granule cells and stunted growth of PC dendrites. Furthermore, trkC and trkB double knockout mice displayed massive cerebellar granule cell death and markedly impaired PC-dendritic differentiation (Minichiello and Klein, 1996). These findings are most likely applicable to the rat cerebellum. However, it should be noted that subtle differences apparently exist between mice and rats regarding the capability of PC to express trkB and trkC (Lindholm *et al*, 1997; Merlio *et al*, 1992). Other factors, such as IGF-I, epidermal growth factor and bFGF have been shown to support granule cell neurogenesis *in vitro* (Gao *et al*, 1991). We did not find statistically significant differences between PTI-NB and control rats with respect to cerebellar expression levels of all the trophic factors investigated. In the cerebellum, IGF-I expression is highest in PC. Therefore, a drop of IGF-I expression as a consequence of PC loss would be predicted. However, since activated Bergmann glia can, most likely, also produce IGF-I in the PTI-NB rat brain, whole cerebellar IGF-I levels might be found to be unchanged when analyzed by RPA.

The statistical data analysis using two-way ANOVA suggested that cerebellar trkC and trkB gene expression levels were first reduced at day 21 p.i., after the onset of BDV-induced granule cell death and the critical postnatal period when granule cell survival depends on PC integrity. ISH studies did not reveal a decrease in cerebellar trkC mRNA transcripts, thus precluding the identification of cells with reduced expression levels of trkC. Reduced cerebellar expression levels of trkC could simply reflect loss of receptor-producing granule and Purkinje cells. However, we did not observe similar reductions in neurotrophin expressions, suggesting that the failure to detect cerebellar cells with reduced trkC mRNA levels might be due to the sensitivity of ISH. Taken together, our data suggest that the reduced cerebellar levels of trkB and trkC receptors most likely do not contribute to granule and/or Purkinje cell death. The implications of reduced cerebellar trkC and trkB levels after day 14 are currently unknown.

Cerebellar damage following pre- or perinatal virus infection has also been demonstrated for other viruses. In some cases, damage has been attributed to immune-mediated lysis of cells, as documented for LCMV (Monjan *et al*, 1974), and reovirus type III (Raine and Fields, 1973). Other mechanisms include lytic viral replication in dividing immature granule cells, as seen in hamsters infected with rat parvovirus (Oster-Granite and Herndon, 1976), or impaired postmitotic granule cell migration, as documented for the Parvovirus minute virus of mice (Ramirez *et al*, 1996), and mumps virus infection of rats (Rubin *et al*, 1998a). The mechanisms of BDV-induced cerebellar damage resemble those operating in neonatal infection of chicken with influenza C virus, characterized by marked

disturbances in dendritic arborization patterns (Parker *et al*, 1994).

There is increasing evidence that neurotrophins and their receptors also play important roles in the processes underlying neuronal plasticity (Thoenen, 1995; McAllister *et al*, 1999). Furthermore, recent evidence indicates that BDNF can cause rapid neuronal membrane depolarization through trkB receptors (Kafitz *et al*, 1999). This finding suggests that the neurotrophin network system can not only modulate but also mediate synaptic transmission. Therefore, BDV-induced changes in the expression of neurotrophin and their receptors could cause altered synaptic function which, in turn, might contribute to neurobehavioral disturbances observed in PTI-NB rats.

While this manuscript was in preparation, a study was published describing spatio-temporal changes in expression of cytokines, apoptosis-related factors and neurotrophic factors in the PTI-NB rat brain (Hornig *et al*, 1999). Our results regarding neurotrophin expression, onset of apoptosis and PC loss are in overall good agreement with this study. However, Hornig *et al*, indicated that, while reduced hippocampal neurotrophin expression was first detected 4 weeks p.i., statistically significant differences were observed only 12 weeks p.i. In contrast, our findings indicate a much earlier onset of statistically significant decreased expression of components of the neurotrophin network, and suggest a possible causal correlation with the neuronal cell loss observed in PTI-NB rats. The discrepancy between the two studies is likely due to the different number of animals analyzed per group and time point (three rats in Hornig *et al*, *versus* five rats in this study). Also, minor genetic differences between Lewis rats substrains (Bender *et al*, 1994) can influence the clinical outcome of viral infections (e.g. Rift Valley fever virus; Michael Frese, Freiburg, personal communication). The Lewis rats and He/80 virus stocks used in the two studies were obtained from different sources. Thus, slight genetic differences possibly affecting both the Lewis rats and virus stocks used might also account for the discrepancies observed within the two studies.

Materials and methods

Virus stocks

The BDV stock used for infection of newborn rats was the fourth brain passage (BDVRp4) in newborn Lewis rats of the Giessen strain He/80 of BDV. BDVRp4 was obtained from rat brain removed 4 weeks post neonatal infection (kindly provided by Oliver Planz and Lothar Stitz, Tübingen). Brains were homogenized into a 10% suspension (wt/vol) in sterile phosphate buffered saline (PBS). After sonication, homogenate was frozen in liquid nitrogen, thawed and centrifuged at 4°C for 5 min (10 000 × g). Aliquots of the supernatant were stored at −70°C. The infectious titer in the supernatant (4×10^5 focus forming units (ffu)/ml) was determined by an immunofocus assay (Herzog and Rott, 1980).

Infection of rats

Pregnant Lewis rats (Charles River, Sulzfeld, Germany) were monitored twice daily. Newborns were inoculated intracranially within 15 h (12 litters) or 23 h (1 litter) after birth with 30 μl of BDVRp4 (ca. 1×10^4 ffu), or with 30 μl of a brain homogenate (10% (wt/vol) suspension in PBS) derived from an adult rat (sham). None of the rats used in the study exhibited symptoms of BD. Consistent with previous reports (Carbone *et al*, 1991; Bautista *et al*, 1994), beginning at day 21 p.i., PTI-NB rats exhibited reduced body weight (17 to 40%) compared to sex and age matched control rats.

Collection and preparation of tissues for histological analysis

Rats were euthanized with CO_2 at different time points p.i. and immediately perfused transcardially with sterile PBS followed by 4% buffered paraformaldehyde (PFA). The brains were removed and postfixed in 4% buffered PFA for 24 h. Brains of rats euthanized at day 8 p.i. were immersion-fixed in 4% buffered PFA for 24 h. After fixation, brains were dehydrated and embedded in paraffin. Eight and 10 μm thick sagittal sections were cut, mounted onto polylysine-coated slides, dried overnight at 37°C and stored at 4°C.

Preparation of RNA

At various time points p.i., rats were euthanized with CO_2. The cerebelli and hippocampi were quickly removed, immediately frozen in liquid nitrogen and stored at −70°C until RNA was prepared. Total RNA was isolated using TRIZOL-reagent method (Life Technologies). Tissue homogenization was done in TRIZOL-reagent by vigorous vortexing and passages through 21G needles. For preparation of hippocampal RNA, glycogen (10 μg) (Roche Molecular Biochemicals) was added to the homogenates as a carrier. RNA samples were dissolved in 0.5 mM EDTA and stored at −70°C.

Plasmid constructs

To generate probes encoding partial sequences of trophic factors and neurotrophin receptors, total RNA was prepared from whole brain of one adult uninfected and BDV-infected rat, as well as from the cerebellum of one adult rat. RNA was reverse transcribed using either random hexanucleotides or oligo(dT). The resulting cDNAs were employed to amplify by PCR fragments of rat neurotrophins β-NGF, NT-3, and BDNF; the growth factors bFGF, rat IGF-I, and rat neurotrophin receptors trkB and trkC, encompassing parts of their respective receptor kinase (trkB-Kin, trkC-Kin) or extracellular domains

(trkC-Ex). PCR was done using specific primers flanked by *Hind*III (sense primer) and *Eco*RI (antisense primer) sites, which allowed subcloning of the amplified DNA fragments into the vector pGEM-3Z (Promega, Madision, WI, USA). The identity of the respective subcloned fragments was verified by sequence analysis. Comparison with published sequences revealed single point mutations in the NGF and BDNF probes, which, however, did not affect their performance in ribonuclease protection assay (RPA). To allow normalization of neurotrophin and neurotrophin receptor mRNA expression, each RPA included a probe for detection of RNA coding for the housekeeping gene ribosomal protein L32. For such purpose, plasmid RPL32N was obtained by cloning of a 99 bp L32-specific fragment from plasmid RPL32 (Sauder and de la Torre, 1999) into pGEM-3Z. Sequence positions and lengths of the subcloned gene fragments, as well as restriction enzymes and polymerases used for generation of antisense and sense RNA probes employed for RPA and *in situ* hybridization studies, are listed in Table 1.

RNase protection assay

To generate a multiprobe set for simultaneous detection of NGF, BDNF, NT-3, bFGF, IGF-I, and L-32 mRNA transcripts, plasmids encoding segments of the respective genes were linearized, purified and adjusted to a concentration of 50 ng/μl. Synthesis of the radiolabeled antisense RPA probe set was done in a volume of 20 μl containing 100 μCi of [α-^{32}P]UTP (3000 Ci/mmol), DTT (200 nmol), transcription buffer (1 $\times$, Promega), 1 μl of template set, rUTP (61 pmol), rGTP, rATP, rCTP (2.75 nmol each), RNase inhibitor (28 U, Pharmacia), and T7 RNA polymerase (20 U, Promega). After 1 h incubation at 37°C, the template DNAs were eliminated by treatment with DNase I (4 U, Ambion) for 30 min at 37°C. After extraction with phenol-chloroform, probes were precipitated with ethanol in the presence of glycogen (20 μg, Roche Molecular Biochemicals) as carrier, dried and dissolved (2.3×10^5 c.p.m./μl) in hybridization buffer (40 mM PIPES (pH 6.4), 0.4 M NaCl, 1 mM EDTA and 80% formamide). Target RNA (10 μg) was dried under vacuum and resuspended in 15 μl of hybridization buffer supplemented with the probe set (4.6×10^5 c.p.m.). Samples were first heated at 93°C for 3–4 min in a heat block, the latter transferred to a hybridization oven and samples hybridized at 56°C for 14–18 h. Unprotected RNA was eliminated by the addition of 280 μl of a mixture containing RNase A (43 μg/ml; Sigma) and RNase T1 (71 U/ml; Ambion) in 375 mM NaCl, 5 mM EDTA, pH 8.0 and 10 mM Tris HCl, pH 7.5–8.0. After 60 min incubation at 30°C, RNases were inactivated for 30 min at 37°C after addition of 30 μl of a mixture containing SDS (6.6%), proteinase K (1.7 mg/ml) and *E. coli* tRNA (330 μg/ml, Roche Molecular Biochemicals). After phenol-chloroform extraction, the protected RNA was precipitated with ethanol, dried, resuspended in loading buffer (80% formamide, 0.1% xylene cyanol, 0.1% bromphenol blue, 2 mM EDTA (pH 8.0)) and analyzed by 8 M Urea-PAGE. Dried gels were first exposed using a phosphoimager and subsequently exposed at -70°C using Biomax films (Kodak). For analysis of trkC-kin, trkC-ex and trkB-kin gene expression, the respective linearized plasmids were mixed with linearized plasmid RPL32N (ca. 250 ng/μl per plasmid). RPA was carried out as described above with the following modifications. For *in vitro* transcription, 35 μCi of [α-^{32}P]UTP (3000 Ci/mmol) and 50 pmol of rUTP were used, and hybridization was done using approximately 3×10^5 c.p.m. of probe.

Immunohistochemistry (IHC)

Sections from paraffin embedded tissue (10 μm) were stained with monoclonal antibody (mAb) Bo18 (kindly provided by Jürgen Richt, Giessen), specific for BDV p40 protein (Haas *et al*, 1986), and a mAb specific for rat calbindin-D28K (Sigma). After deparaffination and rehydration, sections were permeabilized in 0.5% Triton X-100/PBS for 5 min. After washing, slides were blocked in PBS/5% horse serum (v/v) (Vector Laboratories, Burlingame, CA, USA) for 30–60 min at room temperature (RT). Sections were incubated overnight at 4°C with mAbs to Bo18 or to calbindin-D, diluted 1 : 500 or 1 : 200, respectively, in PBS/5% horse serum. Slides were washed and incubated for 30 min at RT with a biotinylated secondary horse, anti-mouse antibody, rat adsorbed (Vector Laboratories), at 1 : 200. Bound antibody was visualized with an avidin-biotin peroxidase kit (ABC; Vector Laboratories) and diaminobenzidine as a substrate. Sections were counterstained with Mayer's hematoxylin (Sigma), dehydrated in graded alcohols and mounted in Entellan (Merck, Darmstadt).

In-situ *hybridization*

In-situ hybridization (ISH) was performed as described by Simmons *et al*. (1989) with some modifications. Briefly, paraffin sections were deparaffinized and rehydrated in graded alcohols. Sections were then postfixed in 4% formaldehyde/PBS, proteinase K treated (2.4 mg/100 ml of 5 $\times$ TE buffer) for 15 min at 37°C, and acetylated (250 μl acetic anhydride in 100 ml PBS) for 10 min. After another 5 min fixation in 4% formaldehyde/PBS, slides were dehydrated in graded alcohols and dried. For synthesis of the sense and antisense trkC-Ex probes, the reaction mixtures (6.26 μl) contained 125 μCi [α-^{33}P]UTP (1000–3000 Ci/mmol), ATP, GTP, CTP (1.55 nmol each), transcription buffer (1 $\times$, Promega), RNase inhibitor (9 U, Pharmacia), SP6 or T7 RNA Polymerase, (7 U each, Promega) and 0.5 μg of

template, linearized with the respective restriction enzyme (Table 1). After incubation at 37°C for 90 min, DNA templates were removed at 37°C (30 min) by addition of DNase I (0.7 U, Ambion). Probes were ethanol precipitated, dried and resuspended in 64 μl of TE buffer containing 28 U of RNasin inhibitor (Pharmacia). Specific activities of the probes were calculated and slides incubated at 56°C overnight in hybridization buffer (100 μl; 50% formamide, 10 mM EDTA, 10% dextran sulfate, 1 × Denhardt's, 10 mM DTT, 2 × SSPE, 100 μg *E. coli* tRNA), containing 25 ng of probe (approximately 1.5×10^7 d.p.m.). After digestion with RNase A (20 μg/ml), slides were washed in decreasing concentrations of SSC and dehydrated in graded alcohols. Dehydrated slides were air dried and exposed for 4 days to Ultra Vision G film (Sterling, Newark, DE, USA). Then, slides were dipped in Kodak NTB-2 emulsion, dried and stored in the dark for 4 weeks. Subsequently, slides were developed, counterstained with Mayer's hematoxylin, mounted and examined by dark and bright field microscopy.

Detection of neuronal cell death in situ
Cells with DNA strand breaks were detected using a TUNEL (terminal deoxynucleotidyl transferase-mediated dUTP nick end labeling) assay (Gavrieli *et al*, 1992). One μM thick sections from paraffin embedded rat brains were deparaffinized and rehydrated in graded alcohols with an incubation step in chloroform for 1 s in-between. Sections were subsequently treated for 7 min at 37°C with PBS/Proteinase K (10 μg/ml), for 30 min at RT in methanol/2.5% H_2O_2 (v/v), and for 20 min at RT in terminal transferase buffer (25 mM Tris, pH 6.6, 200 mM cacodylic acid, 200 mM KCl). Prior and between each of these incubations, the slides were treated twice with PBS/0.3% Triton X-100 at RT for 5 min, each. The tailing reaction was performed for 1 h at 37°C in the presence of tailing buffer (25 mM Tris, pH 6.6, 200 mM cacodylic acid, BSA (0.25 mg/ml)), 1 mM $CoCl_2$, dATP, dCTP, dGTP (20 μM each), dTTP (13 μM), Digoxigenin-dUTP (7 μM) and terminal transferase (0.24 U/μl) (Fermentas, Lithuania). After washes, slides were incubated with PBS/0.3% Triton X-100 twice at 60°C for 5 min and blocked by treatment with 10% fetal calf serum for 15 min at 37°C. Incubation with anti-Digoxigenin antibody, coupled with horseradish-peroxidase (POD), was done at a 1 : 100 dilution in 10% FCS for 30 min at 37°C. Bound antibody was revealed with diaminobenzidine as a substrate and the reaction was stopped after 5 – 15 s by transfer to PBS. Sections were counterstained with hematoxylin, dehydrated and mounted in Entellan. To quantitate the degree of apoptosis in the cerebellar granule layers of both BDV-infected and control rats, numbers of apoptotic cells in at least four microscopic fields per slide were determined (magnification × 250). Two slides per animal were examined, and two BDV-infected and control rats per time point were analyzed. Mean values of apoptotic cells per counted field were calculated.

Statistical analysis
Two-way analysis of variance (ANOVA) with groups (PTI-NB, sham; 2 – 3 animals each per time point analyzed) and days p.i. (8, 14, 21, 27, 33, 48 and 75) as independent factors was employed to calculate group effects for mRNA expression of neurotrophins, growth factors and neurotrophin receptors in the rat cerebellum and hippocampus (α=0.05). Two-way ANOVA with groups (PTI-NB, sham; five animals each per time point analyzed) and days p.i. (14, 21 and 27) as independent factors was employed to calculate group, day, as well as group × day effects for mRNA expression of neurotrophins, growth factors and the trkC-kin neurotrophin receptor in the rat hippocampus (α=0.05). Two-way ANOVA was followed by *post-hoc* one-way ANOVA for pairwise comparisons between infected and noninfected animals at each timepoint, as well as for groupwise comparisons of days.

Software and data processing
Autoradiographs and slides obtained from ISH and IHC studies were scanned using an Agfa scanner (Studio Scan II), or a Nikkon slide scanner (Coolscan 1000), respectively. Composite images were generated using Adobe Photoshop (Adobe Systems, Mountain View, CA, USA) and Microsoft Power Point software. For quantitative analysis of RPA results, dried gels were exposed to phosphoimager plates and quantitations were done using MacBAS2.2 software (Fuji Photo Film Co., Tokyo, Japan). Graphical data were presented using Sigma Plot software (SPSS, Chicago, IL, USA). Statistical analysis was done with procedure GLM of SAS 6.12 software package (Cary, NC, USA).

Acknowledgements

We are grateful to Birgit Scherer for technical assistance, Axel Pagenstecher for help with darkfield microscopy, and Peter Staeheli for helpful discussions. We thank P Staeheli, Otto Haller and Martin Schwemmle for critically reading the manuscript. C Sauder is a fellow of the German Stipendienprogramm Infektionsforschung. Supported by the Deutsche Forschungsgemeinschaft (Sa 682/1-1) and grants NS12428 and MH57063 (JC de la Torre).

References

Bates B, Rios M, Trumpp A, Chen C, Fan G, Bishop JM, Jaenisch R (1999). Neurotrophin-3 is required for proper cerebellar development. *Nat Neurosci* **2:** 115–117.

Bautista JR, Rubin SA, Moran TH, Schwartz GJ, Carbone KM (1995). Developmental injury to the cerebellum following perinatal Borna disease virus infection. *Brain Res Developmental Brain Res* **90:** 45–53.

Bautista JR, Schwartz GJ, de la Torre JC, Moran TH, Carbone KM (1994). Early and persistent abnormalities in rats with neonatally acquired Borna disease virus infection. *Brain Res Bull* **34:** 31–40.

Bender K, Balogh P, Bertrand MF, den Bieman M, von Deimling O, Eghtessadi S, Gutman GA, Hedrich HJ, Hunt SV, Kluge R, Matsumoto K, Moralejo DH, Nagel M, Portal A, Prokop CM, Seibert RT, van Zutphen, LFM (1994). Genetic characterization of inbred strains of the rat (*Rattus norvegicus*). *J Exp Anim Sci* **36:** 151–165.

Breese CR, D'Costa A, Rollins YD, Adams C, Booze RM, Sonntag WE, Leonard S (1996). Expression of insulin-like growth factor-1 (IGF-1) and IGF-binding protein 2 (IGF-BP2) in the hippocampus following cytotoxic lesion of the dentate gyrus. *J Comp Neurol* **369:** 388–404.

Caddy KW, Biscoe TJ (1979). Structural and quantitative studies on the normal C3H and Lurcher mutant mouse. *Philos Trans R Soc Lond B Biol Sci* **287:** 167–201.

Carbone KM, Park SW, Rubin SA, Waltrip II RW, Vogelsang GB (1991). Borna disease: association with a maturation defect in the cellular immune response. *J Virol* **65:** 6154–6164.

Connor B, Dragunow M (1998). The role of neuronal growth factors in neurodegenerative disorders of the human brain. *Brain Res Brain Res Rev* **27:** 1–39.

de la Torre JC (1994). Molecular biology of Borna disease virus: prototype of a new group of animal viruses. *J Virol* **68:** 7669–7675.

Dittrich W, Bode L, Ludwig H, Kao M, Schneider K (1989). Learning deficiencies in Borna disease virus-infected but clinically healthy rats. *Biol Psychiatry* **26:** 818–828.

Dudov KP and Perry RP (1984). The gene family encoding the mouse ribosomal protein L32 contains a uniquely expressed introncontaining gene and an unmutated precessed gene. *Cell* **37:** 457–468.

Eisenman LM, Brothers R, Tran MH, Kean RB, Dickson GM, Dietzschold B, Hooper DC (1999). Neonatal Borna disease virus infection in the rat causes a loss of Purkinje cells in the cerebellum. *J Neurovirol* **5:** 181–189.

Gao WO, Heintz N, Hatten ME (1991). Cerebellar granule cell neurogenesis is regulated by cell-cell interactions in vitro. *Neuron* **6:** 705–715.

Garcia-Estrada J, Garcia-Segura LM, Torres-Aleman I (1992). Expression of insulin-like growth factor I by astrocytes in response to injury. *Brain Res* **592:** 343–347.

Gavrieli Y, Sherman Y, Ben-Sasson SA (1992). Identification of programmed cell death in situ via specific labeling of nuclear DNA fragmentation. *J Cell Biol* **119:** 493–501.

Gonzalez-Dunia D, Sauder C, de la Torre JC (1997). Borna disease virus and the brain. *Brain Res Bull* **44:** 647–664.

Gosztonyi G, Ludwig H (1995). Borna disease – Neuropathology and pathogenesis. In: *Borna disease*. Koprowski H, Lipkin WI, (eds.) Springer: Berlin, pp 39–73.

Gould E, McEwen BS (1993). Neuronal birth and death. *Current Opinion in Neurobiology* **3:** 676–682.

Griffin DE, Hardwick JM (1999). Perspective: virus infections and the death of neurons. *Trends Microbiol* **7:** 155–160.

Haas B, Becht H, Rott R (1986). Purification and properties of an intranuclear virus-specific antigen from tissue infected with Borna disease virus. *J Gen Virol* **67:** 235–241.

Henderson CE (1996). Role of neurotropic factors in neuronal development. *Curr Opin Neurobiol* **6:** 64–70.

Herrup K (1983). Role of staggerer gene in determining cell number in cerebellar cortex. I. Granule cell death is an indirect consequence of staggerer gene action. *Brain Res* **313:** 267–274.

Herzog S, Rott R (1980). Replication of Borna disease virus in cell cultures. *Med Microbiol Immunol* **168:** 153–158.

Hirano N, Kao M, Ludwig H (1983). Persistent, tolerant or subacute infection in Borna disease virus-infected rats. *J Gen Virol* **64:** 1521–1530.

Hornig M, Weissenböck H, Horscroft N, Lipkin WI (1999). An infection-based model of neurodevelopmental damage. *Proc Natl Acad Sci USA* **96:** 12102–12107.

Ip NY, Li Y, Yancopoulos GD, Lindsay RM (1993). Cultured hippocampal neurons show responses to BDNF, NT-3, and NT-4, but not NGF. *J Neurosci* **13:** 3394–3405.

Kafitz KW, Rose CR, Thoenen H, Konnerth A (1999). Neurotrophin-evoked rapid excitation through TrkB receptors. *Nature* **401:** 918–921.

Lewin GR, Barde YA (1996). Physiology of the neurotrophins. *Annual review of Neuroscience* **19:** 289–317.

Lindholm D, Carroll P, Tzimagiogis G, Thoenen H (1996). Autocrine-paracrine regulation of hippocampal neuron survival by IGF-1 and the neurotrophins BDNF, NT-3 and NT-4. *Eur J Neurosci* **8:** 1452–1460.

Lindholm D, Hamner S, Zirrgiebel U (1997). Neurotrophins and cerebellar development. *Perspect Dev Neurobiol* **5:** 83–94.

Lindsay RM, Wiegand SJ, Altar CA, DiStefano PS (1994). Neurotrophic factors: from molecule to man. *Trends in Neurosciences* **17:** 182–190.

Lowenstein DH, Arsenault L (1996). The effects of growth factors on the survival and differentiation of cultured dentate gyrus neurons. *J. Neurosci* **16:** 1759–1769.

Maisonpierre PC, Belluscio L, Squinto S, Ip NY, Furth ME, Lindsay RM, Yancopoulos GD (1990). Neurotrophin-3: a neurotrophic factor related to NGF and BDNF. *Science* **247:** 1446–1451.

Maisonpierre PC, Le Beau MM, Espinosa R, Ip NY, Belluscio L, de la Monte SM, Squinto S, Furth ME, Yancopoulos GD (1991). Human and rat brain-derived neurotrophic factor and neurotrophin-3: gene structures, distributions, and chromosomal localizations. *Genomics* **10:** 558–568.

McAllister AK, Katz LC, Lo DC (1999). Neurotrophins and synaptic plasticity. *Annu Rev Neurosci* **22:** 295–318.

Merlio JP, Ernfors P, Jaber M, Persson H (1992). Molecular cloning of rat trkC and distribution of cells expressing messenger RNAs for members of the trk family in the rat central nervous system. *Neuroscience* **51:** 513–532.

Middlemas DS, Lindberg RA, Hunter T (1991). trkB, a neural receptor protein-tyrosine kinase: evidence for a full-length and two truncated receptors. *Mol Cell Biol* **11:** 143–153.

Minichiello L, Klein R (1996). TrkB and TrkC neurotrophin receptors cooperate in promoting survival of hippocampal and cerebellar granule neurons. *Genes Development* **10:** 2849–2858.

Monjan AA, Cole GA, Nathanson N (1973). Pathogenesis of LCM disease in the rat. In: *Lymphocytic choriomeningitis virus and other arenaviruses*. Lehmann-Grube F, (ed). Springer: New York, pp 195–206.

Monjan AA, Cole GA, Nathanson N (1974). Pathogenesis of cerebellar hypoplasia produced by lymphocytic choriomeningitis virus infection of neonatal rats: protective effect of immunosuppression with antilymphoid serum. *Infect Immun* **10:** 499–502.

Mullen RJ, Eicher EM, Sidman RL (1976). Purkinje cell degeneration, a new neurological mutation in the mouse. *Proc Natl Acad Sci USA* **73:** 208–212.

Murphy LJ, Bell GI, Duckworth ML, Friesen HG (1987). Identification, characterization, and regulation of a rat complementary deoxyribonucleic acid which encodes insulin-like growth factor-I. *Endocrinology* **121:** 684–691.

Narayan O, Herzog S, Frese K, Scheefers H, Rott R (1983). Behavioral disease in rats caused by immunpathological responses to persistent Borna virus in the brain. *Science* **220:** 1401–1403.

Oster-Granite ML, Herndon RM (1976). The development of the cerebellar cortex of the Syrian hamster, Mesocricetus auratus. Foliation, cytoarchitectonic, Golgi, and electron microscopic studies. *J Comp Neurol* **169:** 443–479.

Parker MS, O'Callaghan RJ, Smith DE, Spence HA (1994). The effect of influenza C virus on the Purkinje cells of chick embryo cerebellum. *Int J Dev Neurosci* **12:** 461–470.

Pearce BD, Steffensen SC, Paoletti AD, Henriksen SJ, Buchmeier MJ (1996). Persistent dentate granule cell hyperexcitability after neonatal infection with lymphocytic choriomeningitis virus. *J Neurosci* **16:** 220–228.

Plata-Salaman CR, Ilyin SE, Gayle D, Romanovitch A, Carbone KM (1999). Persistent Borna disease virus infection of neonatal rats causes brain regional changes of mRNAs for cytokines, cytokine receptor components and neuropeptides. *Brain Res Bull* **49:** 441–451.

Pletnikov MV, Rubin SA, Schwartz GJ, Moran TH, Sobotka TJ, Carbone KM (1999a). Persistent neonatal Borna disease virus (BDV) infection of the brain causes chronic emotional abnormalities in adult rats. *Physiol Behav* **66:** 823–831.

Pletnikov MY, Rubin SA, Vasudevan K, Moran TH, Carbone KM (1999b). Developmental brain injury associated with abnormal play behavior in neonatally Borna disease virus-infected Lewis rats: a model of autism. *Behav Brain Res* **100:** 43–50.

Raine CS, Fields BN (1973). Reovirus type 3 encephalitis – a virologic and ultrastructural study. *J Neuropathol Exp Neurol* **32:** 19–33.

Ramirez JC, Fairen A, Almendral JM (1996). Parvovirus minute virus of mice strain i multiplication and pathogenesis in the newborn mouse brain are restricted to proliferative areas and to migratory cerebellar young neurons. *J Virol* **70:** 8109–8116.

Rott R, Becht H (1995). Natural and experimental Borna disease in animals. In: *Borna disease*. Koprowski H, Lipkin WI, (eds). Springer: Berlin, pp 17–30.

Rubin SA, Bautista JR, Moran TH, Schwartz GJ, Carbone KM (1999). Viral teratogenesis: brain developmental damage associated with maturation state at time of infection. *Brain Res Dev Brain Res* **112:** 237–244.

Rubin SA, Pletnikov M, Carbone KM (1998a). Comparison of the neurovirulence of a vaccine and a wild-type mumps virus strain in the developing rat brain. *J Virol* **72:** 8037–8042.

Rubin SA, Sylves P, Vogel M, Pletnikov M, Moran TH, Schwartz GJ, Carbone KM (1998b). Borna disease virus-induced hippocampal dentate gyrus damage is associated with spatial learning and memory deficits. *Brain Res Bull* **48:** 23–30.

Sauder C, de la Torre JC (1999). Cytokine expression in the rat central nervous system following perinatal Borna disease virus infection. *J Neuroimmunol* **96:** 29–45.

Schneemann A, Schneider PA, Lamb RA, Lipkin WI (1995). The remarkable coding strategy of Borna disease virus: a new member of the nonsegmented negative strand RNA viruses (minireview). *Virology* **210:** 1–8.

Schwartz PM, Borghesani PR, Levy RL, Pomeroy SL, Segal RA (1997). Abnormal cerebellar development and foliation in BDNF−/− mice reveals a role for neurotrophins in CNS patterning. *Neuron* **19:** 269–281.

Seay AR, Griffin DE (1981). Effects of viral infections on the developing nervous system. In: *Progress in perinatal neurology*. Korobkin R, Guilleminault C, (eds). Williams and Wilkins: Baltimore, pp 121–155.

Simmons DM, Arriza JL, Swanson LW (1989). A complete protocol for in situ hybridization of messenger RNAs in brain and other tissues with radiolabeled single-stranded RNA probes. *J Histotechnol* **12:** 169–181.

Smeyne RJ, Chu T, Lewin A, Bian F, Crisman S, Kunsch C, Lira SA, Oberdick J (1995). Local control of granule cell generation by cerebellar Purkinje cells. *Mol Cell Neurosci* **6:** 230–251.

Snider WD (1994). Functions of the Neurotrophins during nervous system development: What the knockouts are teaching us. *Cell* **77:** 627–638.

Tessarollo L (1998). Pleiotropic functions of neurotrophins in development. *Cytokine Growth Factor Rev* **9:** 125–137.

Thoenen H (1995). Neurotrophins and neuronal plasticity. *Science* **270:** 593–597.

Tsoulfas P, Soppet D, Escandon E, Tessarollo L, Mendoza-Ramirez JL, Rosenthal A, Nikolics K, Parada LF (1993). The rat trkC locus encodes multiple neurogenic receptors that exhibit differential response to neurotrophin-3 in PC12 cells. *Neuron* **10:** 975–990.

Valenzuela DM, Maisonpierre PC, Glass DJ, Rojas E, Nunez L, Kong Y, Gies DR, Stitt TN, Ip NY, Yancopoulos GD (1993). Alternative forms of rat TrkC with different functional capabilities. *Neuron* **10:** 963–974.

Whittemore SR, Friedman PL, Larhammar D, Persson H, Gonzalez-Carvajal M, Holets VR (1988). Rat beta-nerve growth factor sequence and site of synthesis in the adult hippocampus. *J Neurosci Res* **20:** 403–410.

Wood KA, Dipasquale B, Youle RJ (1993). In situ labeling of granule cells for apoptosis-associated DNA fragmentation reveals different mechanisms of cell loss in developing cerebellum. *Neuron* **11:** 621–632.

Yolken RH, Torrey EF (1995). Viruses, schizophrenia and bipolar disorders. *Clin Microbiol Rev* **8:** 131–145.